



AD-A261 384



NRL/MR/6440-92-7174

**Start-Up Imprinting and Shock Dynamics  
In Laser-Target Interaction**

MARK H. EMERY

*Center for Computational Physics Branch  
Computational Physics and Fluids Dynamics Division*

December 10, 1992

DTIC  
FILED  
FEB 26 1993  
S E D

93-04079



# REPORT DOCUMENTATION PAGE

Form Approved  
OMB No. 0704-0188

Public reporting burden for the collection of information is estimated to average 1 hour per response, including the time for reviewing instructions, searching existing data sources, gathering and maintaining the data needed, and completing and reviewing the collection of information. Send comments regarding this burden estimate or any other aspect of the collection of information, including suggestions for reducing the burden, to Washington Headquarters Service, Directorate for Information Operations and Reports, 1215 Jefferson Davis Highway, Suite 1204, Arlington, VA 22202-4302, and to the Office of Management and Budget, Paperwork Reduction Project (0704-0188), Washington, DC 20503.

1. AGENCY USE ONLY (Leave Blank)	2. REPORT DATE <p style="text-align: center;">December 10, 1992</p>	3. REPORT TYPE AND DATES COVERED <p style="text-align: center;">Interim</p>	
4. TITLE AND SUBTITLE <p style="text-align: center;">Start-Up Imprinting and Shock Dynamics In Laser-Target Interaction</p>			5. FUNDING NUMBERS PE -81103 PR -8068 TA -55 WU -2926A2
6. AUTHOR(S) <p style="text-align: center;">Mark H. Emery</p>			8. PERFORMING ORGANIZATION REPORT NUMBER <p style="text-align: center;">NRL/MR/6440-92-7174</p>
7. PERFORMING ORGANIZATION NAME(S) and ADDRESS(ES) <p style="text-align: center;">Naval Research Laboratory Washington, DC 20375-5320</p>			
9. SPONSORING/MONITORING AGENCY NAME(S) AND ADDRESS(ES) <p style="text-align: center;">Department of Energy Washington, DC 20375-5320</p>			10. SPONSORING/MONITORING AGENCY REPORT NUMBER
11. SUPPLEMENTARY NOTES			
12a. DISTRIBUTION/AVAILABILITY STATEMENT <p style="text-align: center;">Approved for public release; Distribution is unlimited.</p>			12b. DISTRIBUTION CODE
13. ABSTRACT (Maximum 200 words) <p>Improved uniformity of the laser focal spot profile is a necessary criterion for the success of high intensity laser fusion and to improve the quality of data from moderate intensity laser driven shock experiments in solids. Recently developed laser smoothing techniques rely on both temporal smoothing and thermal smoothing to produce uniform ablation pressures on the target surface. Thermal smoothing is not effective during the low intensity portion of a laser pulse and the resultant shock structure mirrors the residual laser nonuniformities. The impact of the first (nonuniform) shock can be diminished by using foam layers, a precursor x-ray flash, shallow angles of incidence, and by adiabatically compressing the target with a temporally long, slowly rising laser pulse.</p>			
14. SUBJECT TERMS <p>Start-up imprinting                      laser generated shocks                      induced spatial incoherence laser inhomogeneities                      thermal smoothing</p>			15. NUMBER OF PAGES <p style="text-align: center;">27</p>
17. SECURITY CLASSIFICATION OF REPORT <p style="text-align: center;">UNCLASSIFIED</p>			16. PRICE CODE
18. SECURITY CLASSIFICATION OF THIS PAGE <p style="text-align: center;">UNCLASSIFIED</p>	19. SECURITY CLASSIFICATION OF ABSTRACT <p style="text-align: center;">UNCLASSIFIED</p>	20. LIMITATION OF ABSTRACT <p style="text-align: center;">UL</p>	

# CONTENTS

**I. INTRODUCTION** ..... 1

**II. RESULTS** ..... 3

**III. SUMMARY AND CONCLUSIONS** ..... 10

**ACKNOWLEDGEMENTS** ..... 11

**REFERENCES** ..... 12

Accession For	
NTIS - CRA&I	<input checked="" type="checkbox"/>
UIIC - IAS	<input type="checkbox"/>
UIIC - OIC/I	<input type="checkbox"/>
JPL Center	
By	
Distribution/	
Availability Codes	
Dist	Avail and/or Special
<b>A-1</b>	

# START-UP IMPRINTING AND SHOCK DYNAMICS IN LASER-TARGET INTERACTION

## I. Introduction

A high degree of ablation pressure uniformity is a necessary criterion for the success of laser-driven inertial confinement fusion. Asymmetries in the ablation pressure must remain less than a few percent throughout the implosion process if high gain is to be achieved.<sup>1</sup> This places a severe requirement on the uniformity of the laser beam since thermal diffusion is only effective at reducing those spatial nonuniformities with scalelengths smaller than the separation distance between the absorption and the ablation region.<sup>2</sup> With short laser wavelengths, required for good laser-target coupling<sup>3</sup>, thermal diffusion is ineffective at reducing all but the highest spatial frequency nonuniformities. The ability of the recently developed random phase plate (RPP)<sup>4</sup>, smoothing by spectral dispersion (SSD)<sup>5</sup>, and induced spatial incoherence (ISI)<sup>6</sup> laser smoothing techniques to produce a nearly uniform ablation pressure is strongly contingent on the degree of thermal smoothing in the ablating plasma.<sup>6,7</sup> The SSD and ISI techniques benefit from temporal smoothing as a result of the broadband nature of the laser light but residual nonuniformities persist with all three methods. Nearly all shaped reactor-like laser pulses are composed of four distinct phases: (1) an initial rapid rise to a low - to - moderate intensity, (2) a long temporal, low intensity "foot", (3) a moderately rapid (power law-like) rise to high intensity, and (4) the main drive portion of the pulse. See Figure 1. The first two regimes are usually referred to as the start-up phase, and the ratio of the final drive power to the foot power is termed

the dynamic range. The details of the actual pulse shape (initial rise time, duration of the "foot", dynamic range, and final drive intensity) are dictated by the target design (material composition, layered/nonlayered, target thickness) and the desired final velocity of the target; but, in general, the pulse is designed so that the initial shock keeps the target on a low adiabat and breaks out through the rear of the target as the laser intensity reaches the beginning of the drive portion of the pulse.

Thermal smoothing is not effective at reducing any inherent laser beam nonuniformities during the "foot" portion of the pulse and the shock structure generated during the start-up phase will mirror any residual laser nonuniformities.<sup>7</sup> The resulting small initial mass perturbations can grow linearly a order of magnitude or more, depending on the target thickness, as a result of the Richtmyer-Meshkov instability<sup>8</sup> before the target begins the rapid acceleration phase.<sup>7</sup> The shocks produced during the start-up phase can be the determining factor in the success or failure of the implosion process as it is the mass variations near the beginning of the drive portion of the laser pulse which will provide the seeds for Rayleigh-Taylor<sup>9</sup> (RT) growth during the acceleration phase. For a target to implode uniformly, the mass variations at this point in time must be  $\ll 1\%$ .

We present the results from a series of numerical simulations using the FAST2D Laser Matter Interaction Model<sup>7</sup>; and, in particular, we investigate two facets of the start-up problem. We investigate the impact of a shaped, reactor-like, ISI-smoothed laser beam on thick (100's of microns), solid DT and layered DT targets; and, we investigate the impact

of an ISI-smoothed laser beam on CH targets with target thicknesses and pulse shapes similar to those envisioned for the NIKE Laser System<sup>10</sup>.

## II. Results

For most of the results presented here, we modeled the laser profile with a 20 x 20 echelon array with  $d_{00} = 320 \mu m$  and a laser coherence time  $t_c = 1 ps$ .  $d_{00}$  is the effective laser spot size. The laser wavelength is  $0.264 \mu m$ . This corresponds to a lens with an  $F_{number} = 32$ . The laser spot is flat over the distance  $d_{00}$ . The transverse dimension is  $160 \mu m$ , represented by 80 zones, and there are 120 zones in the longitudinal direction. The ISI mode spectrum ranges between  $8 \mu m$  and  $160 \mu m$ . This compares favorably with the envisioned reactor-like parameters :  $F_{number} \approx 30$ ,  $d_{00} = 600 \mu m$  and a 60 x 60 echelon array. These conditions produce an ISI spectrum ranging between  $5 \mu m$  and  $300 \mu m$ .

The instantaneous incident ISI laser profile exhibits large amplitude randomly fluctuating structures as shown in Figure 2a. The long time average behavior ( $100 t_c$ ) still exhibits some residual structure as shown in Figure 2b. Figure 2c shows the time averaged incident laser profile after  $1000 t_c$ ;  $\sigma_{RMS} = 0.037$  with a maximum amplitude variation of  $\pm 8.6\%$ . These residual structures can be reduced in magnitude by lateral thermal smoothing as long as the distance between the ablation region and the laser absorption region is larger than the scalelengths of the residual laser asymmetries. To test this hypothesis, we generated a moderately long scalelength plasma with a "perfect" laser beam before impacting the target with an ISI-smoothed laser beam. The temporal pulse shape is shown

in Figure 3a. The laser light is spatially uniform until 6 nsec, at which time the ISI spectrum is "turned on". Nearly all of the laser energy is absorbed between the 1/4 critical density ( $15 \mu m$  from the target surface) and critical density ( $1 \mu m$  from the target surface) surfaces. Figure 3d shows the isodensity contours of an  $80 \mu m$  thick CH target at 16 nsec. The target is quite uniform well into the rapid acceleration phase. The mass perturbation at 16 nsec is  $\Delta m/m \approx 0.2\%$ . This density profile is to be contrasted with the case of a "frozen-in" 4:1 sinusoidal laser asymmetry shown in Figure 3b at 9.5 nsec. The initial conditions are the same as the ISI case. A similar result is obtained with an ISI-like beam with zero bandwidth, a rough approximation to an RPP. In this case, at 6 nsec, the uniform laser profile shifts to a "frozen-in" ISI-profile. The target density contours are shown in Figure 3c at 11 nsec.

The ability of the ISI concept to produce a smooth ablation pressure is based on a combination of temporal smoothing (over 100's of  $t_c$ ) and transverse thermal smoothing. Transverse thermal conduction is difficult to achieve with a reactor-like shaped laser pulse because of the long, low intensity "foot" prior to the main driving beam. The isodensity contours for a  $330 \mu m$  thick frozen DT target illuminated with a shaped ISI laser beam is shown in Figure 4 at 12 nsec. At this time the target mass variation ( $\Delta(\rho r)/\langle \rho r \rangle$ ) is 22%. Early in the laser pulse, the laser energy is deposited directly onto the target surface. The highly nonuniform nature of the ISI beam results in spatially and temporally nonuniform shocks traversing the target. The target surface, itself, is perturbed and as the shock passes through the target it leaves residual mass perturbations in its wake. These residual

variations grow linearly in time, in a Richtmyer-Meshkov-like manner, as the target drifts with a nearly constant velocity. Although it appears that a long pulse ISI laser beam may severely perturb an ICF target, this should be contrasted with the impact of a temporally equivalent laser pulse with a "frozen-in" 4:1 sinusoidal asymmetry. In this case, the laser asymmetry is imposed at  $t = 0$  and the mass variation is greater than 2:1 at 8 nsec.

Several target designs were investigated in an attempt to mitigate the impact of the initial nonuniform shock structure. In one case, a 180  $\mu\text{m}$  thick solid DT target with a 100  $\mu\text{m}$  thick low density ( $0.08 \text{ gm/cm}^3$ ) DT layer was used. This layer reduces the perturbation on the shock front to some degree before the shock impacts the frozen DT target. The mass variation at 15 nsec is 21%. In order to model layered, dissimilar materials, we incorporated a volume fraction method into the FAST2D Model. Figure 5 is an  $x - t$  diagram, isodensity contours of each material (spatially separated for visual clarity), illustrating the shock structure stemming from a typical power law laser pulse impacting a layered target of 200  $\mu\text{m}$  frozen DT ( $0.201 \text{ gm/cm}^3$ ), 30  $\mu\text{m}$  CH ( $1.04 \text{ gm/cm}^3$ ) and 100  $\mu\text{m}$  DT foam ( $0.08 \text{ gm/cm}^3$ ). The initial shock strikes the foam-CH interface at 5 nsec, sending a transmitted shock through the CH and a reflected shock back through the foam. The reflected shock strikes the free surface of the foam sending a rarefaction through the foam at about the same time (7 nsec) the transmitted shock strikes the CH-DT interface, sending a transmitted shock through the DT fuel and a rarefaction back through the CH. These rarefactions decompress the target by about a factor of 2. The rarefaction strikes the CH-foam interface (10 nsec) sending another shock through the CH and subsequently

through the DT fuel (12 nsec). The combination of the foam-CH layers eliminates most of the short wavelength mode structure stemming from the ISI beam and diminishes the mass perturbation,  $\Delta(\rho r)/\langle\rho r\rangle = 17\%$  at the peak of the laser pulse (15 nsec). This perturbation level is reduced to 9% by tailoring the laser pulse to rise somewhat more rapidly to eliminate the effect of the rarefaction. To investigate in more detail the effect of the shock-rarefaction structure on a material interface, we simulated a spatially uniform laser pulse, with a temporal profile as above, impacting a DT-CH-foam target with a 2  $\mu\text{m}$  sinusoidal perturbation of the CH-foam interface. The temporal evolution (Figure 6) of this perturbation shows 4 phases of growth. The first shock strikes the CH-foam interface at 5 nsec and the perturbation grows with a linear RM growth rate of  $7.8 \times 10^4$  cm/s ( $\dot{r}_{theory} = 7.6 \times 10^4$  cm/s), until 7.5 nsec when the rarefaction propagates through the CH layer rapidly increasing the spatial extent of the interface perturbation (there is no change in  $\Delta\rho r$  during this period). As the second shock compresses the CH layer the growth stops (11 nsec) and the phase of the perturbation is reversed (13 nsec). These results indicate that layered, multimaterial targets are beneficial in the sense that they can mitigate the impact of the initial shock structure; however, the temporal shape of the laser pulse must be more finely tailored to counteract the rarefaction stemming from the fuel-ablator interface.

The ablation to absorption distance can be increased by using longer wavelength laser light which would also result in an increase in the amount of thermal smoothing. However, longer wavelength laser light implies poorer laser-target coupling and reduced efficiency.<sup>3</sup>

By combining long wavelength laser light at the beginning of the pulse with short wavelength laser light during the compression and acceleration phases, thermal smoothing would be enhanced during the early phase of the pulse and laser-target coupling would be enhanced during the acceleration phase. Using the same multilayer target discussed above, the first 8 ns of the laser beam is modeled as 1.054  $\mu\text{m}$  ISI laser light ( $t_c=1$  ps) which then smoothly evolves, over 1.5 ns, to 0.264  $\mu\text{m}$  ISI laser light ( $t_c=1$  ps) for the rest of the laser pulse. At 15 ns,  $\Delta(\rho r)/\langle\rho r\rangle = 4\%$ . The perturbation amplitude at this time includes  $\approx 1.5$  e-foldings of RT growth. At 12 ns,  $\Delta(\rho r)/\langle\rho r\rangle = 0.9\%$ . Modeling the first 8 ns of the 1.054  $\mu\text{m}$  beam as being perfectly uniform results in a mass variation of only 1.8% at 15 ns (0.4% at 12 ns). These perturbation levels are still too large to enable the target to implode uniformly.

In the absence of a "perfect" laser beam, a uniform blowoff plasma could be generated by coating the target with a thin (O(few 100  $\text{\AA}$ )) high-Z material and striking the target with a very short burst of x-rays. We have approximated this interaction by depositing 1/4 J of energy directly onto the surface of a frozen DT target during a 250 ps FWHM pulse. The target is 330  $\mu\text{m}$  thick. This energy pulse produces a very weak shock, O(10's of kbar), and at 10 ns after the "x-ray flash", the density scalelength, at critical density for 1/4  $\mu\text{m}$  laser light, is  $\approx 100\mu\text{m}$ . The target is then illuminated with a 0.264  $\mu\text{m}$  ISI - smoothed laser beam at a 30° angle of incidence (with respect to the normal). For this case, the laser pulse has a 5 ns Gaussian rise to an intensity of  $10^{12}$  W/cm<sup>2</sup> which then evolves into a power law pulse which peaks at  $3 \times 10^{14}$  W/cm<sup>2</sup> at 15 ns. A plot of the rays

incident at an angle of  $30^\circ$  at the peak of the laser pulse is shown in Figure 7a. The turning point of the rays is just outside of the critical surface and the plasma continues to absorb energy from the rays until each ray contains  $< 1\%$  of its initial energy. The maximum mass variation of the target,  $\Delta(\rho r)/\langle \rho r \rangle$ , is 4.8 % at 15 ns. The mass perturbations are larger than the layered, multiple laser wavelength cases, but significantly smaller than the nonlayered, normal incident cases. Figure 7b illustrates the rays at the same time and angle of incidence as above but without the initial "x-ray flash". Note that there appears to be some evidence for self-focusing.

The results of this series of calculations is summarized in Figure 8 in the form of a histogram. The maximum mass perturbation level (in per cent) and the time at which perturbation level is measured are denoted as well as the target and laser pulse characteristics. These numerical results indicate that cold, low density foam layers, multiple wavelength lasers and initial x-ray flashes can significantly reduce the mass perturbation level stemming from the initial imprint of an ISI-smoothed laser beam. There is also experimental evidence that an initial x-ray flash can eliminate plasma jetting generated by the initial imprint of an ISI-smoothed laser.<sup>11</sup> The numerical results, however, indicate that the perturbation level at the beginning of the drive portion of the pulse (several percent) is still too large to enable the target to implode uniformly. Since it is the first shock which is the culprit here, it may be possible to compress the target adiabatically - without any shocks except for the final drive portion of the pulse - and circumvent the problem. This would entail a very long, slowly rising laser pulse. A pulse of this shape

would generate kilobar-like pressures in the target and thus compressive stress, shear stress, elastic response and plastic flow become important considerations. We have developed an elastic-plastic-hydrodynamic numerical model<sup>12</sup> to account for these phenomena and now apply this model to the study of an ISI-smoothed laser pulse on targets similar to those envisioned for the initial set of experiments for the NIKE Laser System.

For the first case, the ISI-smoothed laser pulse has the canonical power-law profile with a 1/2 nsec rise to  $10^{12}$  W/cm<sup>2</sup>, a  $t^{-5/4}$  rise to  $3 \times 10^{14}$  W/cm<sup>2</sup> at 6 nsec, followed by a 3 nsec drive at this intensity. See Figure 1. The target is 60  $\mu$ m of CH, and the laser wavelength is 1/4  $\mu$ m with a coherence time of 1 psec. The target mass variation at the beginning of the drive portion of the pulse (6 nsec) is 3.6%. This is comparable to the mass variation (3.8%) attained with the pure hydrodynamic version of the code under the same pulse shape conditions. This is to be expected as the first shock stemming from this laser pulse is  $O(1$  Mbar) and the elasticity/plasticity of the material does not play a role. The target would soon fracture as a result of the RT instability with an initial mass perturbation of this magnitude. The total energy density of the laser pulse (9 nsec) is 970 kJ/cm<sup>2</sup> and the target velocity at 9 nsec is  $2.5 \times 10^7$  cm/s.

For the shock-free pulse, the laser intensity starts at  $10^7$  W/cm<sup>2</sup> and increases very slowly reaching  $3 \times 10^{14}$  W/cm<sup>2</sup> at 28 nsec. See Figure 9a. Shown in Figure 9b is an  $x - t - \rho$  plot illustrating the target response. A small compression wave begins propagating through the target at  $\approx 20$  nsec; the total stress has reached an amplitude of  $\approx 20$  kbar at this time. The peak compressed density is 8.2 gm/cm<sup>3</sup> which is 12% larger than for

the 6 nsec pulse case. Figure 10 illustrates the target isodensity contours at 28 nsec - the beginning of the drive portion of the pulse. The amplitude of the maximum density variation is only 0.5%. This is close to the requirement ( $O(0.1\%)$ ) for uniform implosion. Note that a portion of this growth (an e-folding or so) is due to RT growth as the target begins to rapidly accelerate at  $\approx 27$  nsec. For this case, the total energy density of the laser pulse (31 nsec) is  $1200 \text{ kJ/cm}^2$  and the target velocity at 31 nsec is  $2 \times 10^7 \text{ cm/s}$ .

A KrF laser system can be susceptible to a very low intensity, temporally long prepulse. We have examined the consequences of this prepulse on the subsequent target response. We model the prepulse with an 200 ns pulse with a constant intensity of  $10^7 \text{ W/cm}^2$ . The laser intensity is strong enough to send weak elastic compression/tension waves through the target but does not damage or weaken the target. The elastic waves produce a weak erosion on both the front and rear surface of the target. See Figure 11. When this target is impacted with either the canonical power-law pulse or the adiabatic pulse, there is little discernable difference in the results as compared to the cold target response.

### III. Summary and Conclusions

In summary, we have shown that it is possible to influence the impact of the residual nonuniformities inherent in a nonperfect laser beam during the start-up phase. Cold, low density layers, multiple laser wavelengths, shallow angles of incidence, and thin high-Z ablaters can all significantly reduce the perturbations stemming from an imperfect laser beam. The perturbation level may be minimized by eliminating the first shock in the laser pulse by designing a temporally long, slowly rising, truly adiabatic laser pulse. A small

price is paid in laser energy and hydrodynamic efficiency, but the net result is that the perturbation level is reduced by nearly an order of magnitude below the level attained with the canonical power-law pulse or with other target designs.

### **Acknowledgements**

The author gratefully acknowledges fruitful discussions with J. Gardner, R. Lelunberg and S. Obenschain. This work was supported by the US DoE and ONR.

## REFERENCES

1. S. E. Bodner. *J. Fusion Energy* **1**, 221(1981).
2. M. H. Emery, J. H. Orens, J. H. Gardner, and J. P. Boris, *Phys. Rev. Lett.* **48**, 253(1982).
3. J. H. Gardner, and S. E. Bodner, *Phys. Rev. Lett.* **47**, 1137 (1981).
4. Y. Kato, K. Mima, N. Miyanaga, S. Arinaga, Y. Kitagawa, M. Nakatsuka, and C. Yamanaka, *Phys. Rev. Lett.* **53**, 1057(1984).
5. S. Skupsky, R. W. Short, T. Kessler, R. S. Craxton, S. Letzring, and J. M. Soures, *J. Appl. Phys.* **66**, 3456 (1989).
6. R. H. Lehmberg and S. P. Obenschain, *Opt. Commun.* **46**, 27(1983); R. H. Lehmberg, A. J. Schmitt, and S. E. Bodner, *J. App. Phys.* **62**, 2680 (1987).
7. M. H. Emery, J. H. Gardner, R. H. Lehmberg. and S. P. Obenschain, *Phys. Fluids B* **3**, 2640 (1992).
8. R. D. Richtmyer, *Commun. Pure Appl. Math.* **13**, 297 (1960); Ye. Ye. Meshkov, NASA Technical Translation NASA TT F-13, 074 (1970).

9. Lord Rayleigh, *Theory of Sound*, 2nd. ed. (Dover, New York, 1945. Vol. 2); G. I. Taylor, Proc. R. Soc. London Ser. A **201**, 192 (1950).
10. J. H. Gardner, J. P. Dahlburg, M. H. Emery, and S. E. Bodner, Bull. Am. Phys. Soc. **35**, 1969(1990).
11. M. Desselberger, T. Afshar-rad, F. Khattak, S. Viana, and O. Willi, Phys. Rev. Lett. **68**, 1539 (1992).
12. M. H. Emery and J. H. Gardner, sub. to Phys. Fl. B.

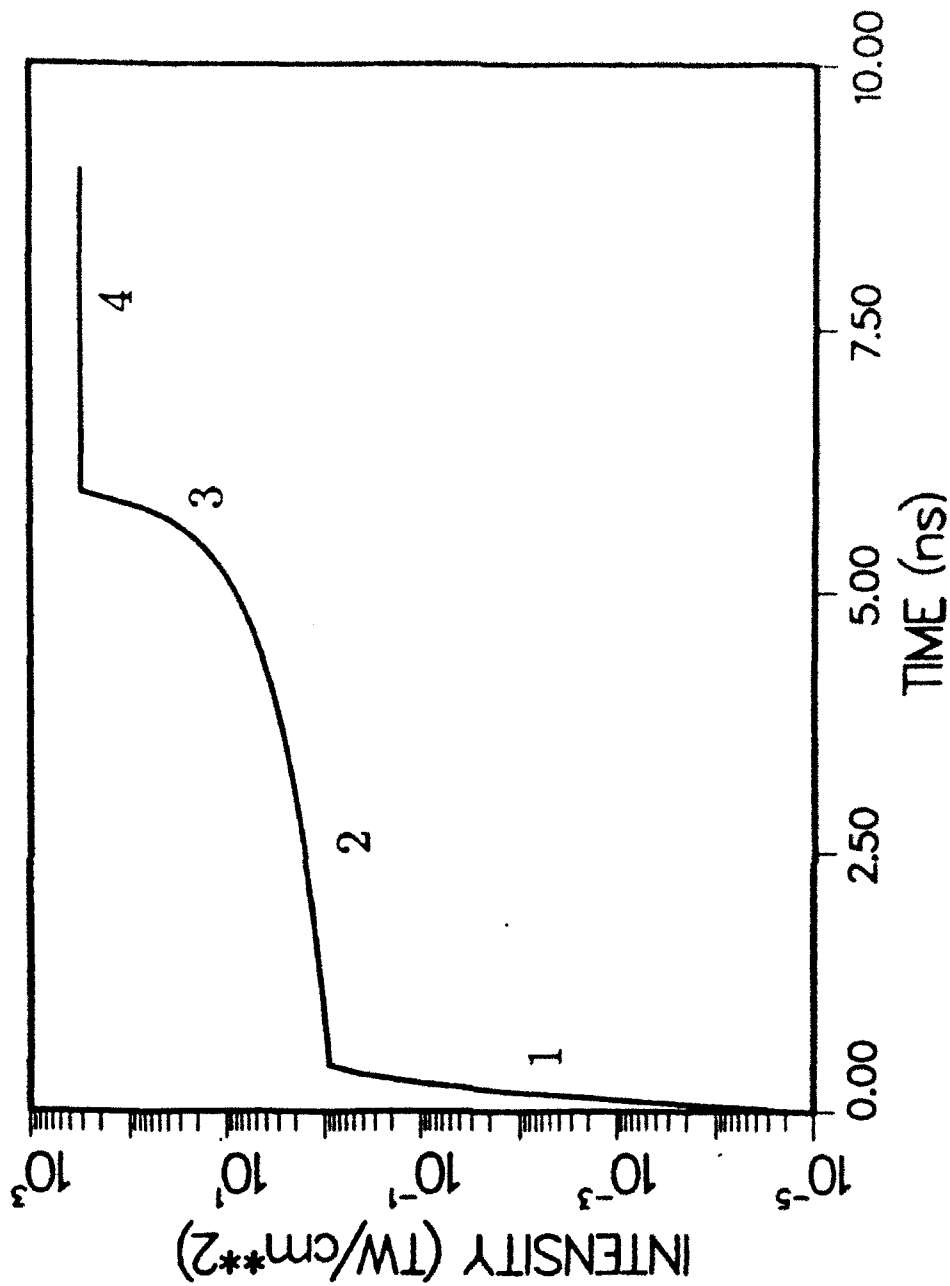
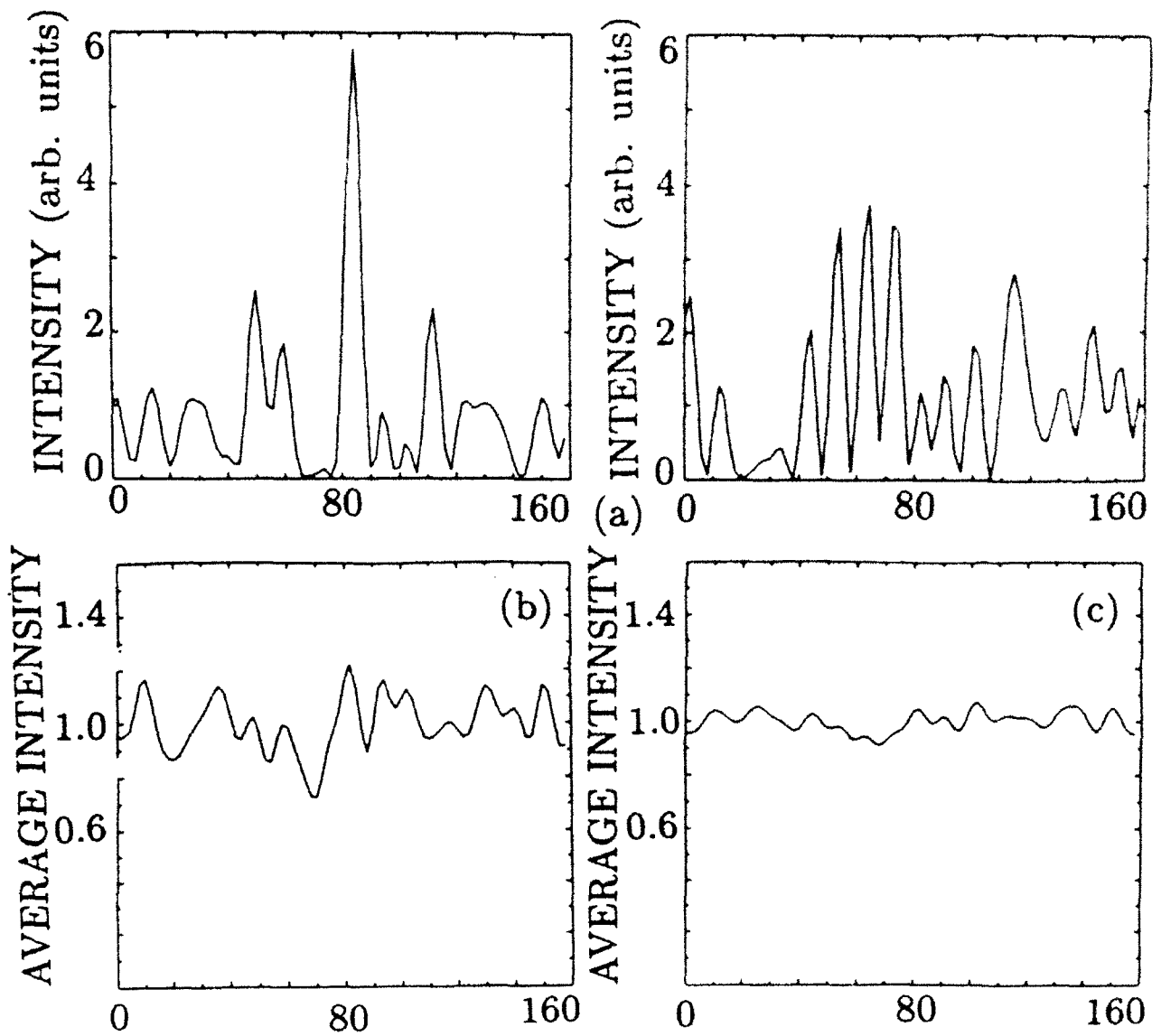


Figure 1. Plot of the intensity versus time of a typical power law laser pulse. The sections labeled

1 and 2 are the startup portion of the pulse, the drive portion of the pulse is labeled 4.

This pulse shape is the canonical power law pulse for the NIKE Laser System.



**Figure 2.** (a) Instantaneous ISI laser intensity versus transverse dimension ( $\mu m$ ) at 2 different times. Laser intensity averaged over (b) 100  $t_c$ , (c) 1000  $t_c$ .

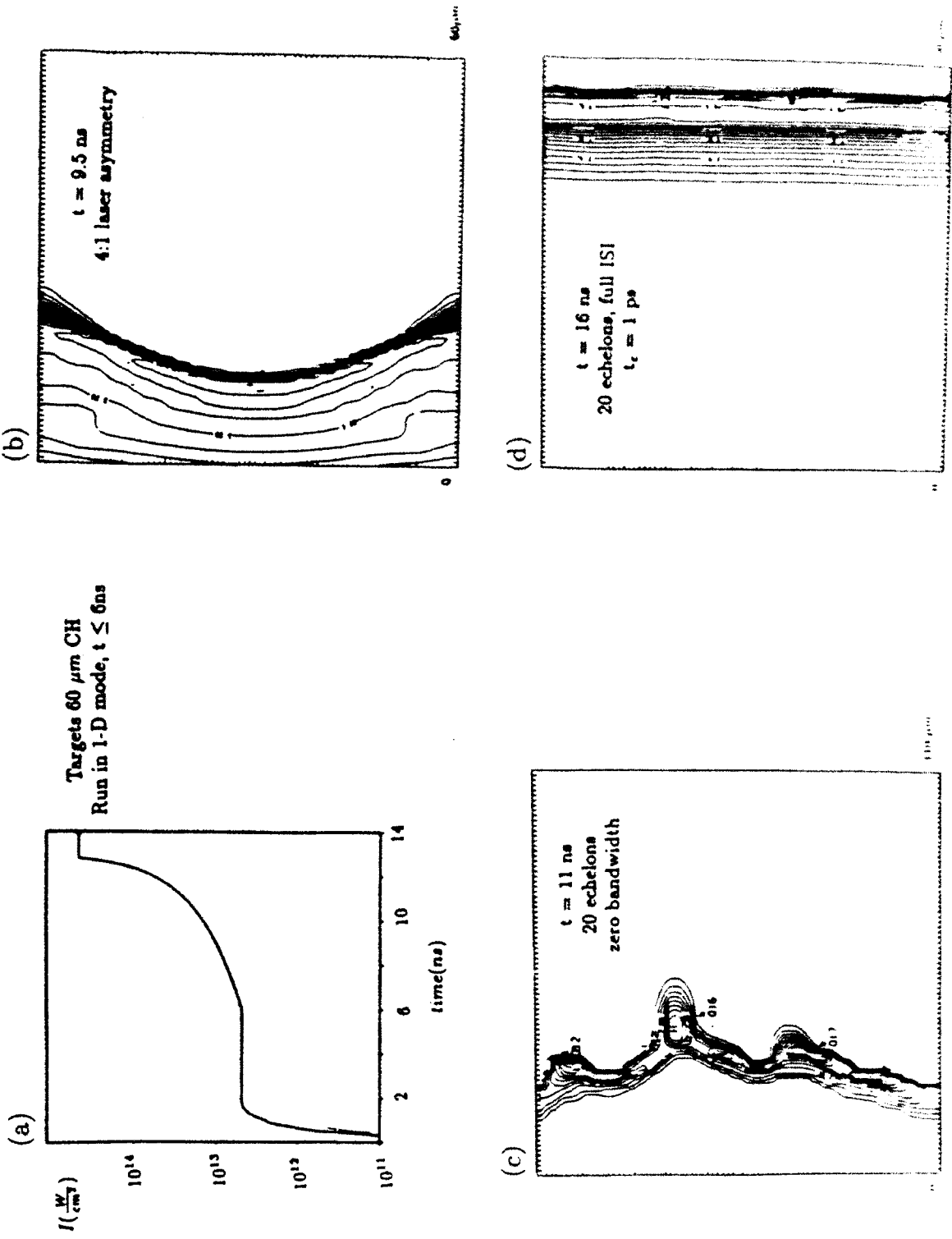


Figure 3. (a) Canonical power law laser profile. Isodensity contours responding to (b) 4:1 laser asymmetry, (c) RPP laser pulse, (d) ISI laser pulse.

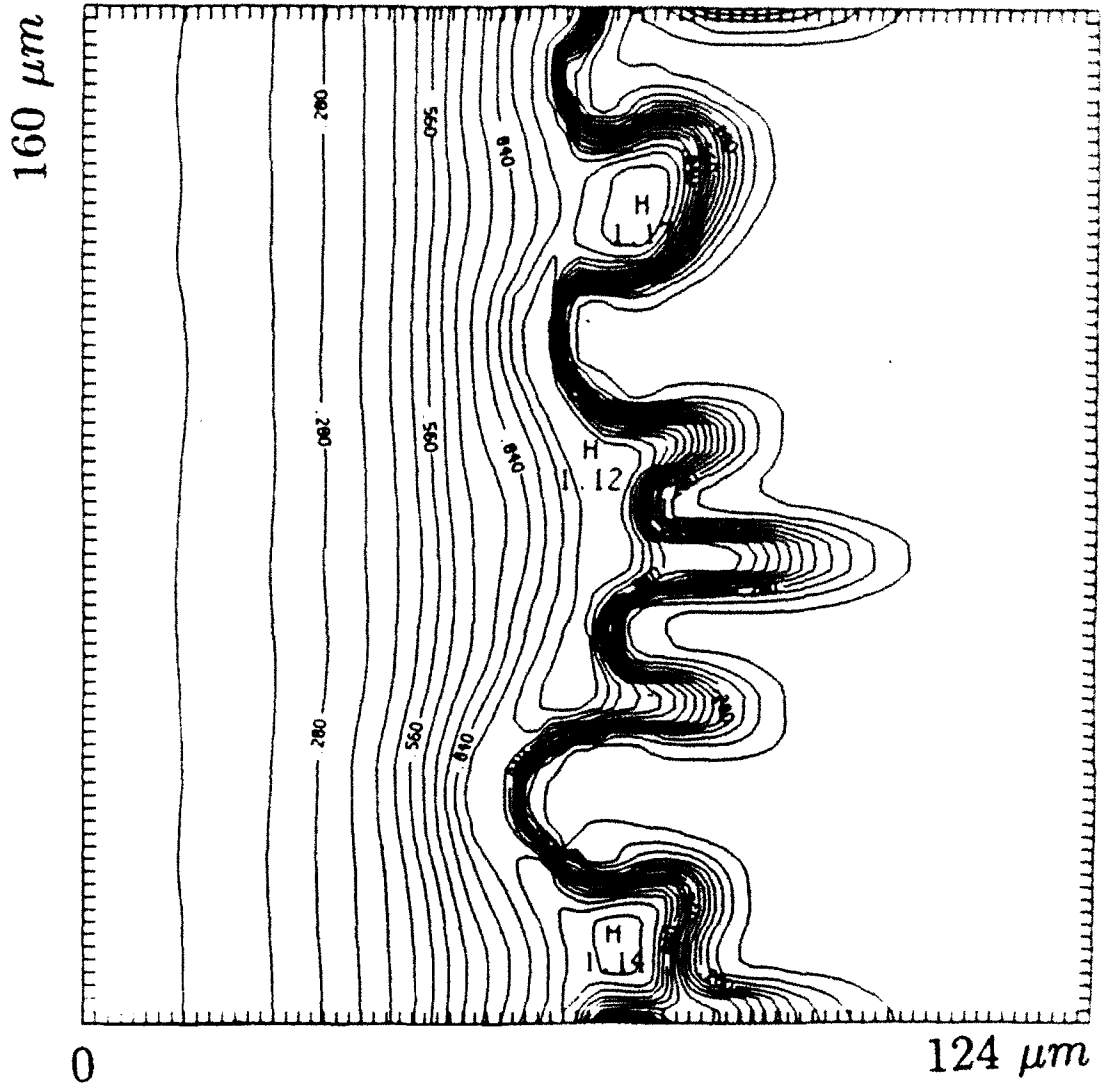


Figure 4. Isodensity contours at 12 nsec for  $300 \mu\text{m}$  DT target illuminated with ISI laser beam.

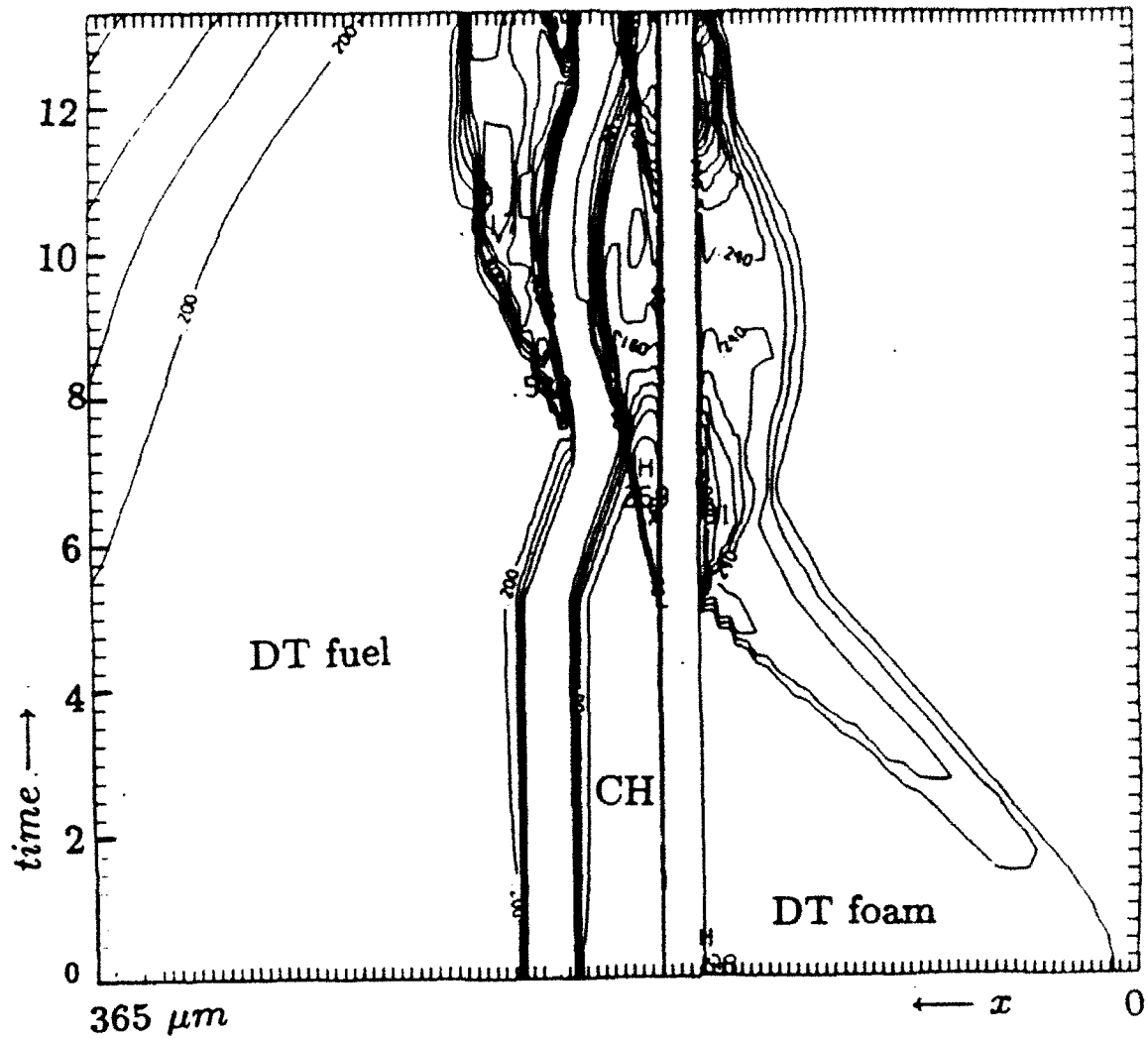
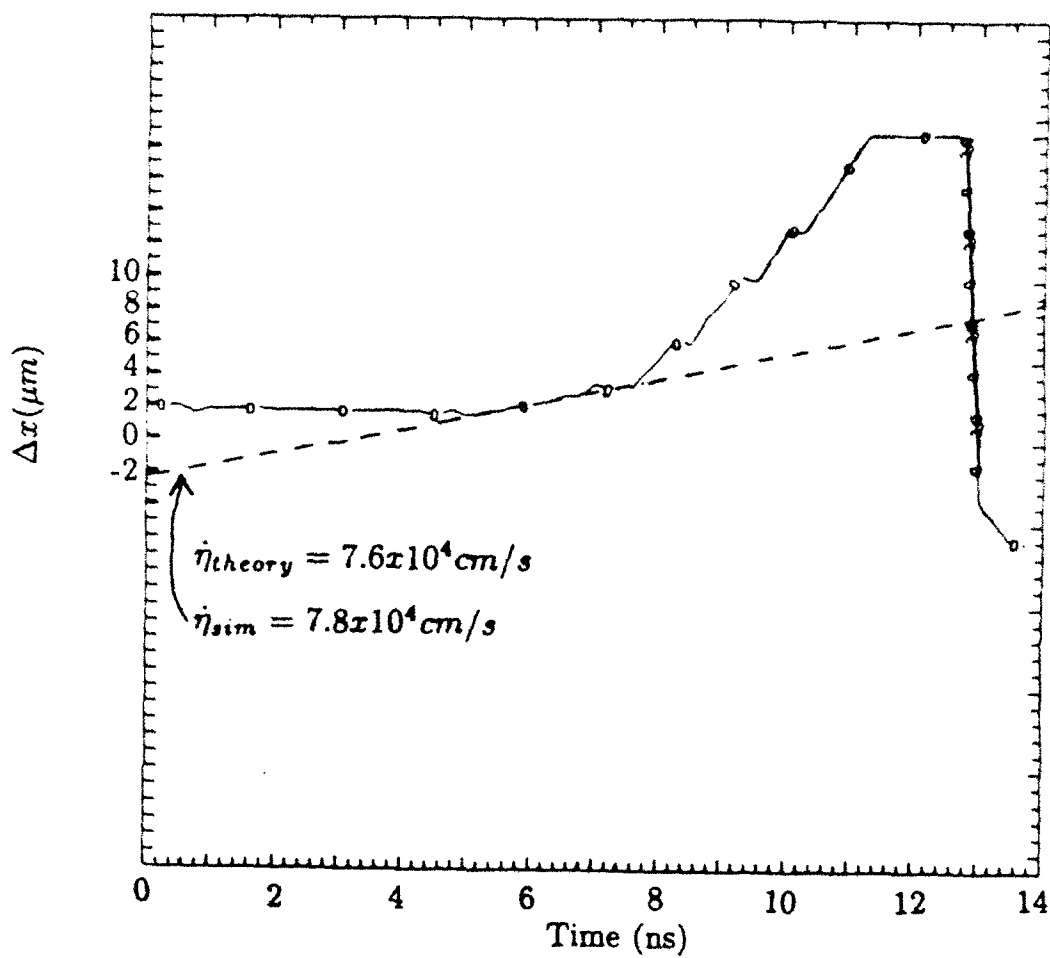
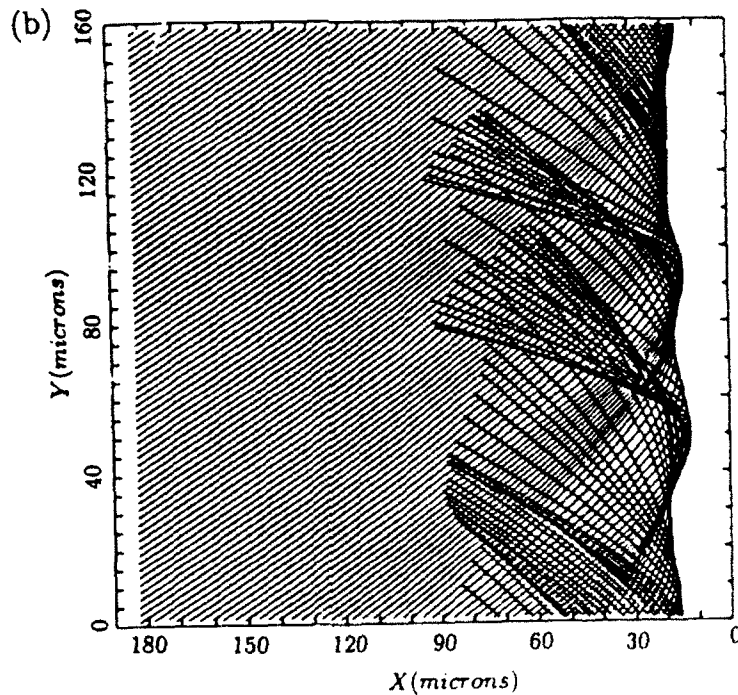
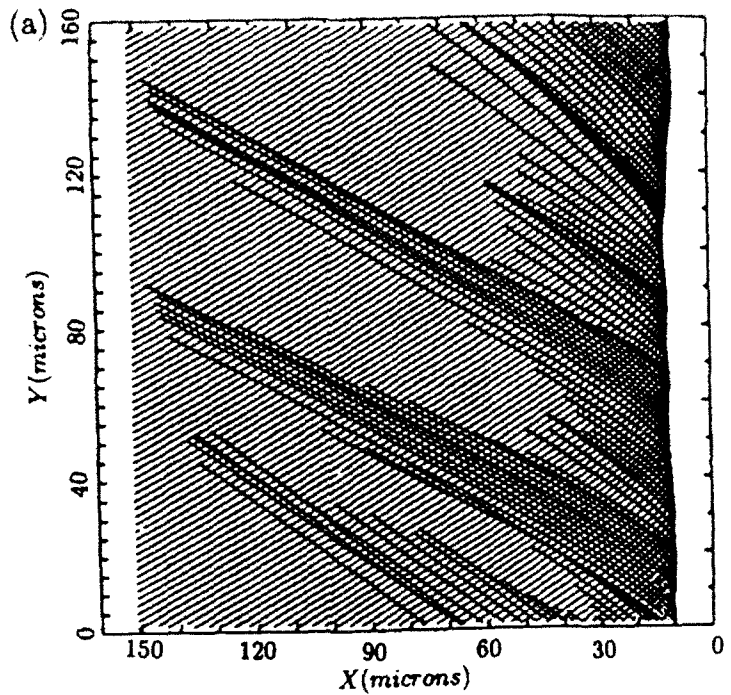


Figure 5.  $x - t$  diagram, resulting from 1-D averaged isodensity contours in the center-of-mass frame, showing shock evolution in layered target.



**Figure 6.** Temporal evolution of perturbation on CH-Foam interface in response to power law shock structure.



**Figure 7.** (a) Plot of the rays incident at an angle of  $30^\circ$  on a  $330 \mu\text{m}$  thick DT target at the peak of the laser pulse after the target was illuminated with an artificial "x-ray flash". (b) Plot of the rays at the same angle of incidence and at the same time as (a) but without the "x-ray flash". Note that there is some evidence for self-focusing.

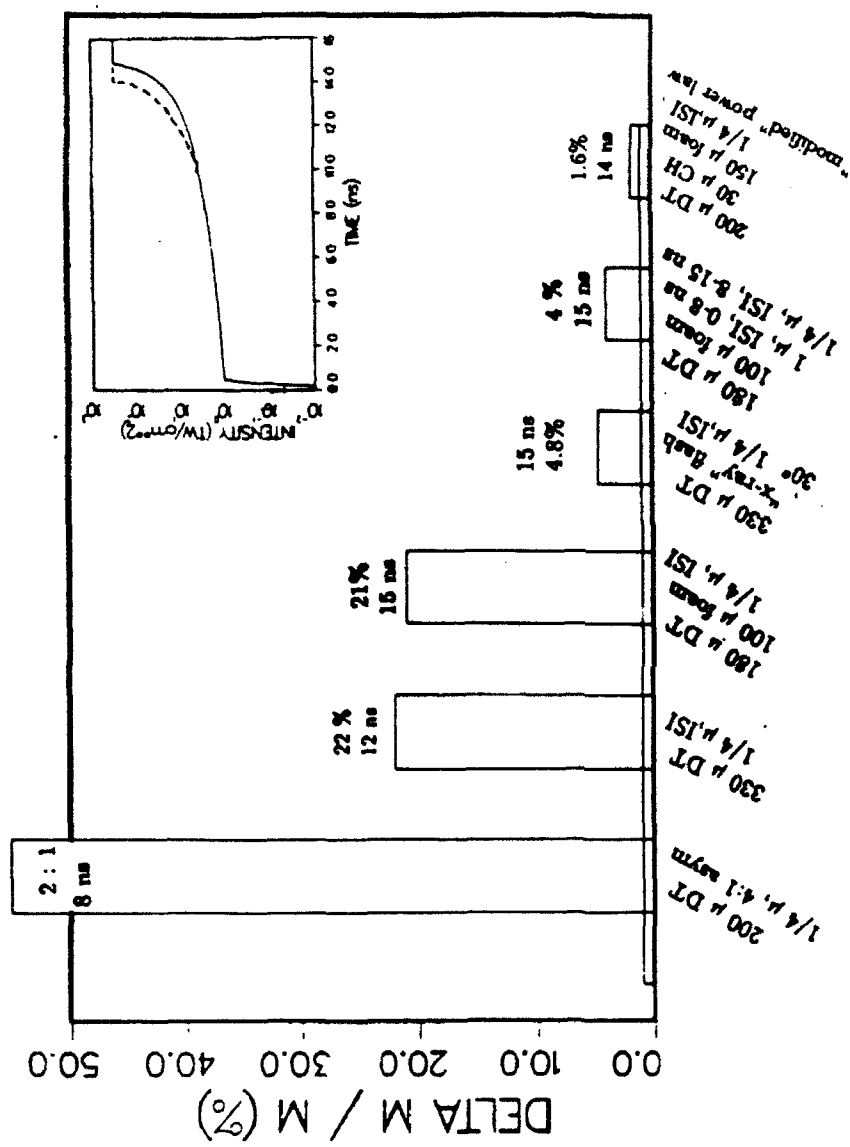


Figure 8. Histogram comparing the mass perturbation levels for various target designs and laser scenarios using a 15 ns shaped ISI laser pulse. The dashed line illustrates the "modified" laser pulse.

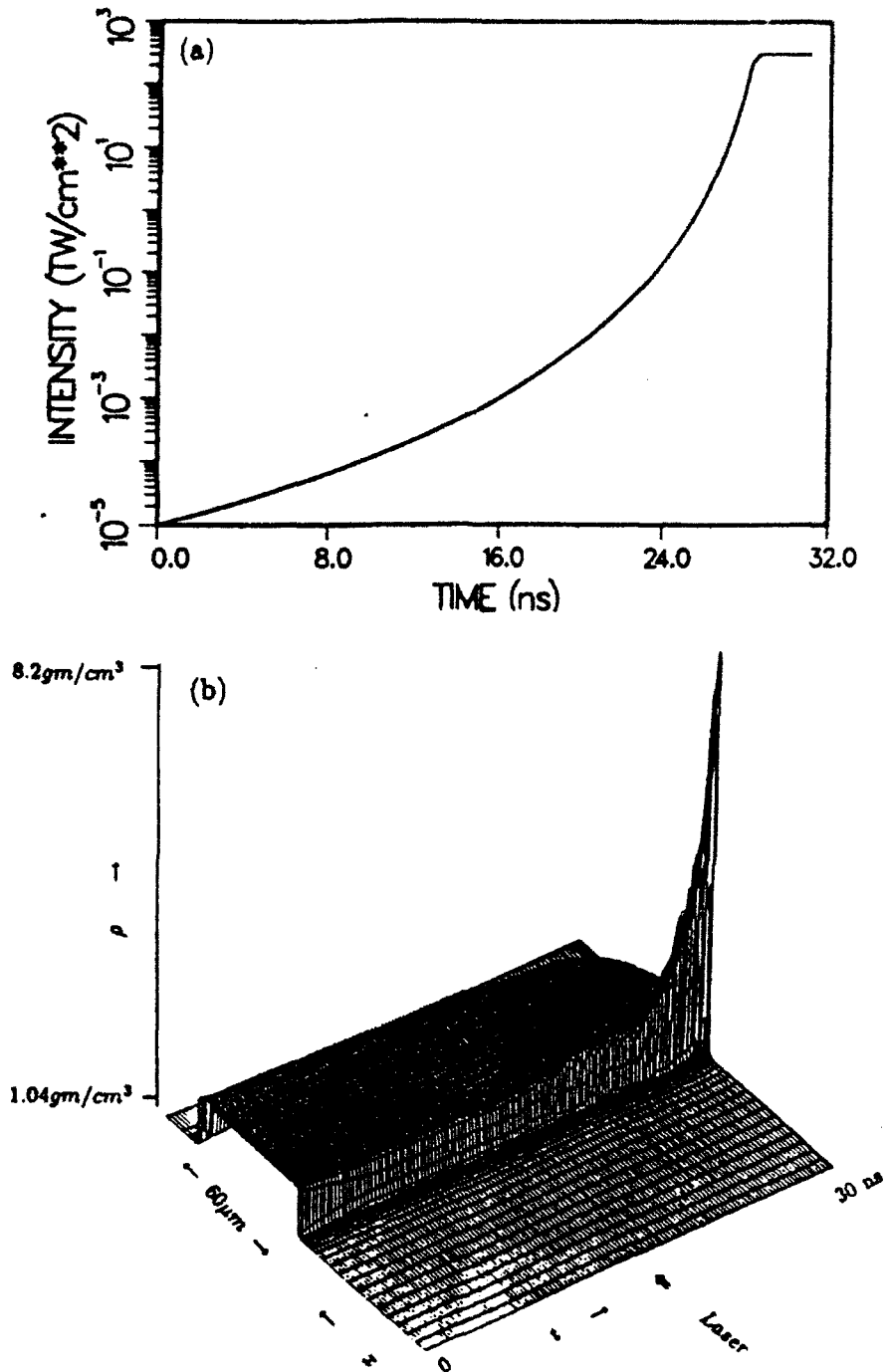


Figure 9. (a) Intensity profile for the temporally long, slowly rising laser pulse. (b)  $x$ - $t$ - $\rho$  plot for the  $60 \mu\text{m}$  thick plastic target (in the center-of-mass frame) for the slowly rising laser pulse.

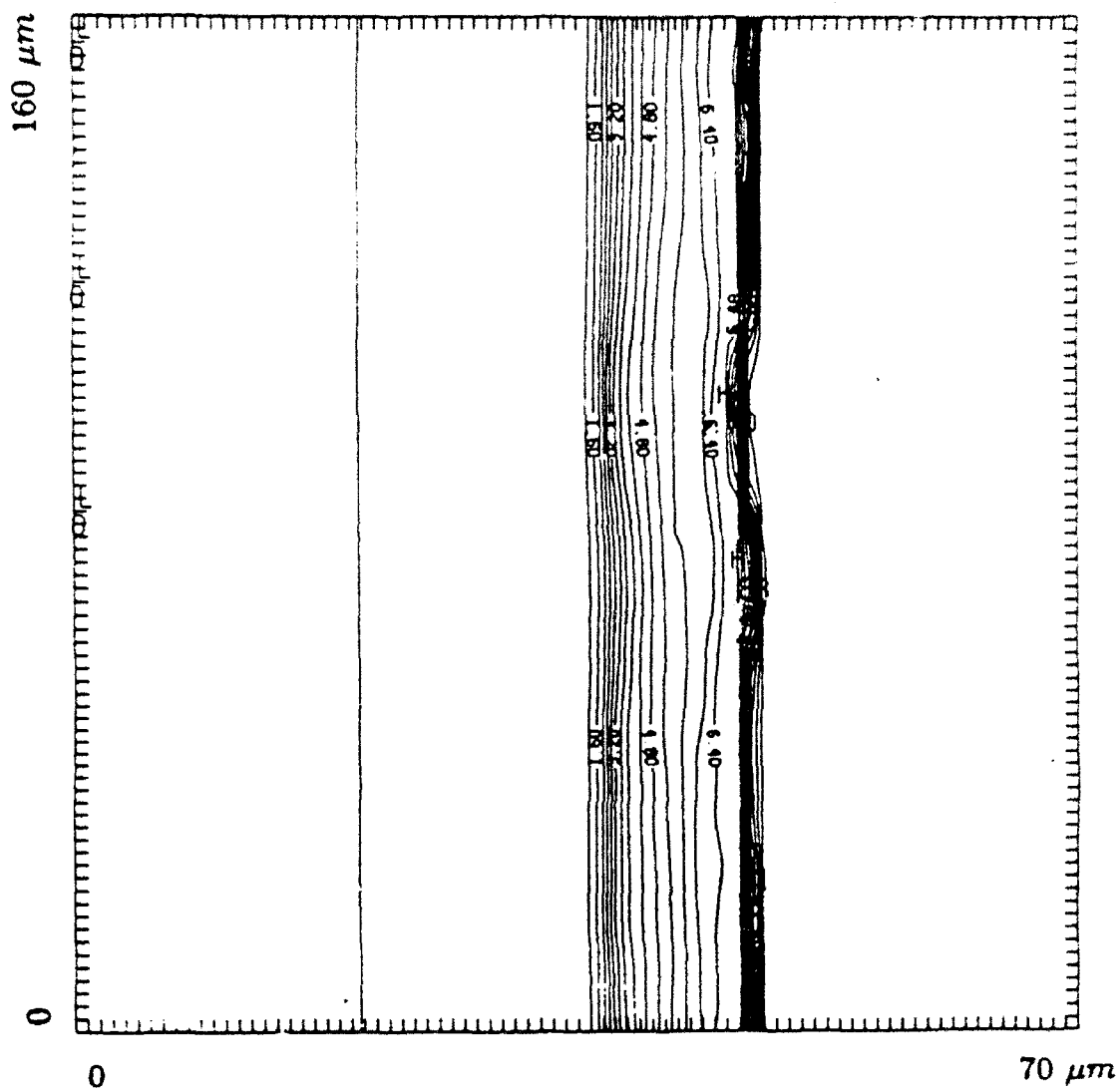
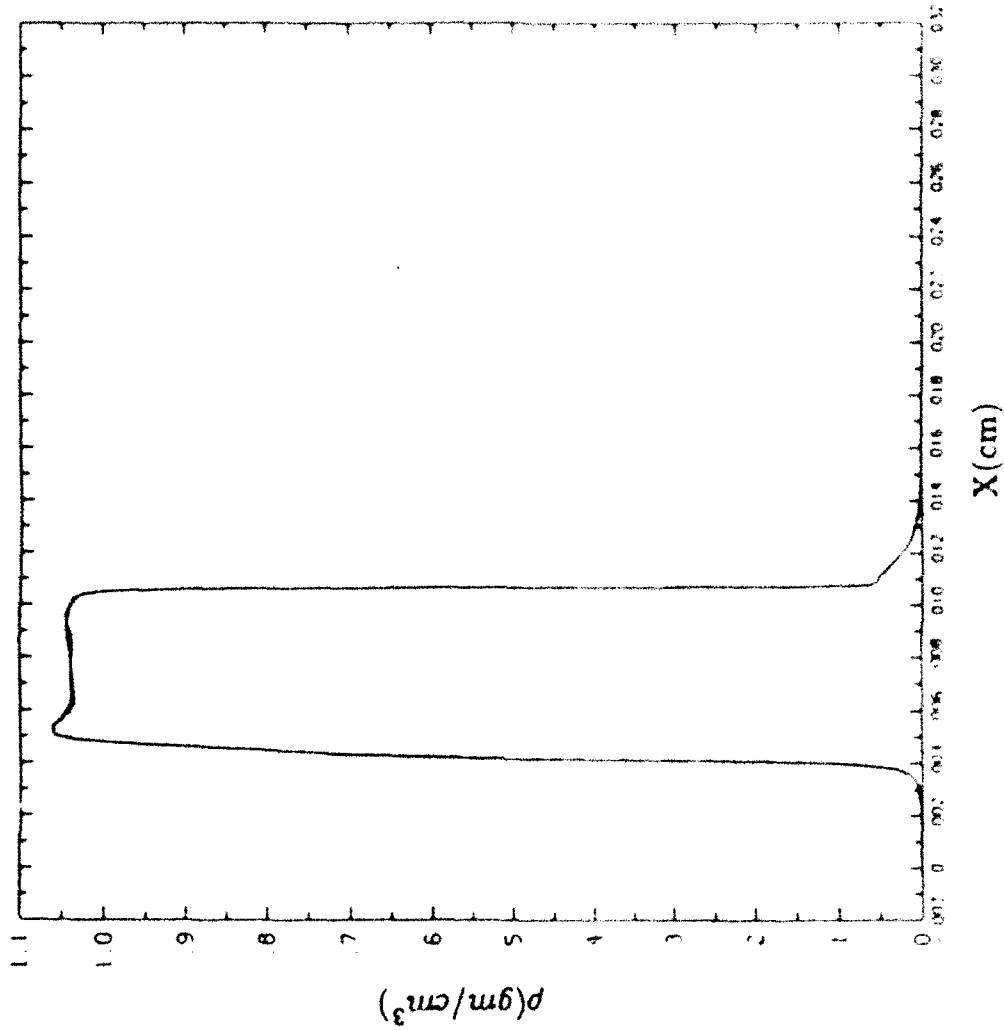


Figure 10. Isodensity contours of the 60  $\mu\text{m}$  thick CH target at 28 nsec impacted with the slowly rising laser pulse. The maximum mass variation at this time is 0.5%.



**Figure 11.** Density profile of a 60 μm thick CH target after illumination with a laser at  $10^{17}$  W/cm<sup>2</sup> for 200 nsec.